Aerosol influence on radiative cooling

By HARTMUT GRASSL, *Institut für Meteorologie, University of Mainz, Germany*

(Manuscript received October 30, 1972; revised version February 26, 1973)

ABSTRACT

Aerosol particles have a complex index of refraction and therefore contribute to atmospheric emission and radiative cooling rates. In this paper calculations of the longwave flux divergence within the atmosphere at different heights are presented including water vapour and aerosol particles as emitters and absorbers. The spectral region covered is 5 to 100 microns divided into 23 spectral intervals. The relevant properties of the aerosol particles, the single scattering albedo and the extinction coefficient, were first calculated by Mie-theory and later by an approximation formula with a complex index of refraction given by Volz. The particle growth with relative humidity is also incorporated for different aerosol types and size distributions. These values were taken from Hänel. The results show a significant contribution of aerosol particles to longwave flux divergence, although strongly dependent on the imaginary part of the refractive index, the size distribution and relative humidity. The aerosol contribution to radiative cooling becomes very important in layers below temperature inversions, which are barriers for particle diffusion. There exist atmospheric conditions where the aerosol contribution to radiative cooling is as large as cooling by water vapour.

Introduction

Aerosol particles have a complex index of refraction and contribute to atmospheric absorption and emission and therefore to radiative heating or cooling. The aerosol influence on the heat budget is however still unknown. The work described in this paper is restricted to the longwave region of the spectrum from 5 to 100 microns wavelength. Probably the first to postulate an absorption coefficient or a complex index of refraction for atmospheric aerosols was Waldram (1945). Later several other workers could only account for discrepancies between measurements and calculations of sky emission or continuum absorption in the wavelength region of 8 to 13 microns by introducing a hypothetic aerosol absorption coefficient. At present nearly all researchers assume absorption by atmospheric aerosols but they can only employ estimated values. Recently Fischer (1970) and Volz (1972) gave first results for aerosol absorption coefficients in the visible and infrared region. Volz however could only use the part of atmospheric aerosols which could be sampled from natural precipitation.

The calculations of longwave fluxes by radiation charts and also of the flux divergence by means of differences of these fluxes are strongly disagreeing. Earlier investigations where the influence of atmospheric aerosols have been included were performed by Zdunkowski (1972), Joseph (1971) and Atwater (1971). However, Zdunkowski and Joseph used the refractive index of water. Atwater employed various values of the imaginary part, since the imaginary part was completely unknown.

Therefore these papers can only be regarded as a first approximation. Within the last two years Hänel (1970, 1972) has given the first results of the dependence of particle radius on relative humidity which are also incorporated in the following calculation procedure.

Calculation procedure

1. *Principles*

For all calculations horizontal homogeneity is assumed. There are two possible ways for the calculation of heating or cooling rates. First we can determine the spectral flux divergence dF_λ/dh from the difference of the net flux F_λ

at two different heights h_1 and h_2. The net flux F_{λ,h_i} at the height h_i was calculated following equations (1) and (2).

$$F_{\lambda,h_i} = F_{\downarrow h_i} + F_{\uparrow h_i} \tag{1}$$

where $F_{\downarrow h_i}$ is the downward and $F_{\uparrow h_i}$ the upward hemispheric flux at hight h_i.

$$\begin{aligned} F_{\lambda,h_i} &= -\int_0^{\pi}\int_{h_i}^{\infty} k_\lambda^v B_\lambda(T_h) \exp\left(-\int_{h_i}^{h} k_\lambda^v/\cos\varphi\, dh\right) dh\, d\varphi \\ &+ \int_0^{\pi} B_\lambda(T_g) \exp\left(-\int_{h_i}^{0} k_\lambda^v/\cos\varphi\, dh\right) \cos\varphi\, d\varphi \\ &+ \int_0^{\pi}\int_{h_i}^{\infty} k_\lambda^v B_\lambda(T_h) \\ &\times \exp\left(-\int_{h_i}^{h} k_\lambda^v/\cos\varphi\, dh\right) dh\, d\varphi \end{aligned} \tag{2}$$

with k_λ^v = volume absorption coefficient at wavelength λ
$B_\lambda(T_h)$ = spectral Planck's function at temperature T_h
T_g = ground temperature
φ = distance from the vertical.

For more than one absorber the spectral volume absorption coefficient k_λ^v can be written as the sum of water vapour absorption coefficient k_λ^v and of the aerosol absorption coefficient k_λ^a.

The spectral longwave flux divergence dF_λ/dh is then determined from the difference of the net flux in two heights.

$$\Delta F_\lambda/\Delta h = (F_{\lambda,h_2} - F_{\lambda,h_1})/(h_2 - h_1) \tag{3}$$

This flux divergence is only a mean value for an atmospheric layer.

In another method the flux divergence dF_λ/dh is determined from the difference between the entire radiation $I_\lambda = \int_{4\pi} I_\lambda(\omega)\, d\omega$ arriving at a height h_i and the blackbody radiation $B_\lambda(T_{h_i})$ multiplied by the volume extinction coefficient.

$$dF_{\lambda,h_i}/dh = k_\lambda^v(I_\lambda - B_\lambda(T_{h_i})) \tag{4}$$

By using equation (4) flux divergence is determined for a distinct height. In the present calculations both methods were used for the 8–13 micrometer region. Obviously the flux divergence dF_λ/dh in the infrared is the difference between two nearly equal terms and therefore the accuracy of the calculations should be as high as possible, especially for thin layers with the first method and for regions with large optical depths with the second method. Both ways show good agreement for a mean value of one layer in the region 8–13 micrometer. The numerical integration over wavelength was achieved by dividing the entire region into 23 intervals sufficiently broad to diminish computing time yet sufficiently small to avoid greater variations of Planck's function within the interval using the values given by Rodgers and Walshaw (1966). They applied the statistical band model to water vapour line data. Integration over zenith distance was done by summing over 10 intervals with $|\cos\varphi_i - \cos\varphi_{i+1}| = 0.1$. In test calculations a further subdivision was shown not to be necessary. The flux divergence dF/dh was converted into cooling rates, dT/dt, in °C per unit time following equation (5)

$$dT/dt = 1/\varrho c_p \cdot dF/dh \tag{5}$$

with ϱ = air density and c_p = specific heat at constant pressure.

2. *Representation of calculation parameters*

The atmosphere was first divided into 16 layers 250 to 2 000 m thick up to 16 km. In special programs the lowest layers were again divided in several sublayers to show the details within temperature inversions or near the ground. The wavelength region covered is 5 to 100 microns or 2 000 to 100 wavenumbers.

In the window region from 8–13 microns water vapour absorption was treated as a continuum absorption using values given by Bignell (1963). No attempt was made to include a so-called *e*-type absorption of water vapour so far only measured in the laboratory (Bignell, 1970). The water vapour absorption coefficients within the 6.3 micron and the rotation band were taken from Rodgers (1966). He used Goody's statistical band model to determine transmission functions in broad spectral intervals. The pressure and temperature dependence was also taken from Rodgers (1966). The ozone band at 9.6 microns was included at first, but contribution to longwave flux divergence near the ground, where aerosol influence is strongest, was so small and only slightly height dependent, that the calculations could be simplified by omitting ozone contribution. No attempt was made to include the 15 micron band

21533490, 1973, 4, Downloaded from https://onlinelibrary.wiley.com/doi/10.1111/j.2153-3490.1973.tb00622.x by MPI 348 Meteorology, Wiley Online Library on [05/07/2023]. See the Terms and Conditions (https://onlinelibrary.wiley.com/terms-and-conditions) on Wiley Online Library for rules of use; OA articles are governed by the applicable Creative Commons License

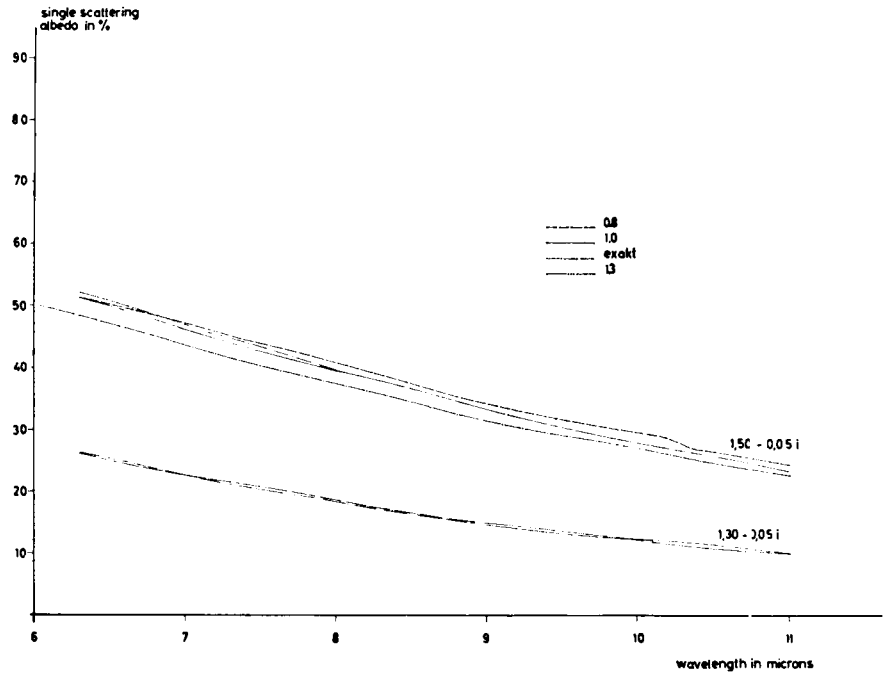

Fig. 1. Accuracy of the approximation formula for the determination of the single scattering albedo for different complex indices of refraction. The numbers 0.8, 1.0, 1.3 refer to those values of $\alpha = 2\pi r/\lambda$ where approximation for small particles after Penndorf (1962) was replaced by the method of Deirmendjian (1960).

Table 1*a*. *Size distributions used within the following calculations*

Name	Number density
Haze C	$n(r) = 4.97 \cdot 10^6 \cdot r^2 \exp(-15.1186\sqrt{r})$
Haze M	$n(r) = 5.33 \cdot 10^4 \cdot r \exp(-8.944\sqrt{r})$
Junge	$n(r) \sim r^{-4}$ within the range 0.01 – 10 microns
M Junge	Measured upon the German research vessel Meteor on the Atlantic by Jaenicke et al. (1971).

of carbon dioxide, since it was found that the aerosol contribution below 8 and above 13 microns was negligible because the absorption coefficient of water vapour far exceeded the aerosol absorption coefficient. From other calculations it has been shown that carbon dioxide has no significant contribution to longwave radiative cooling within the lower troposphere except within the lowest few meters (Zdunkowski, 1972).

The necessary aerosol input parameters for the model were size distribution (see Table 1*a*), complex index of refraction (see Table 1*b*) and the variations of these two parameters with relative humidity. From the size distribution and the complex index of refraction the single scattering albedo $\omega_0 = Q_{sca}/Q_{ext}$ and the spectral volume extinction coefficient k_λ were first determined by Mie-theory calculations for different wavelengths within the region 5 to 100 microns.

Later an approximation formula for the ex-

Table 1*b*. *Imaginary part of refractive index depending from wavelength (mean value of all given numbers by Volz (1972) for all samples taken at Mainz)*

Wavelength in microns	8.0	8.8	9.3	10.1	11.0	12.0	13.0
Imaginary part	0.13	0.30	0.20	0.13	0.05	0.05	0,05

21533490, 1973, 4, Downloaded from https://onlinelibrary.wiley.com/doi/10.1111/j.2153-3490.1973.tb00622.x by MPI 348 Meteorology, Wiley Online Library on [05/07/2023]. See the Terms and Conditions (https://onlinelibrary.wiley.com/terms-and-conditions) on Wiley Online Library for rules of use; OA articles are governed by the applicable Creative Commons License

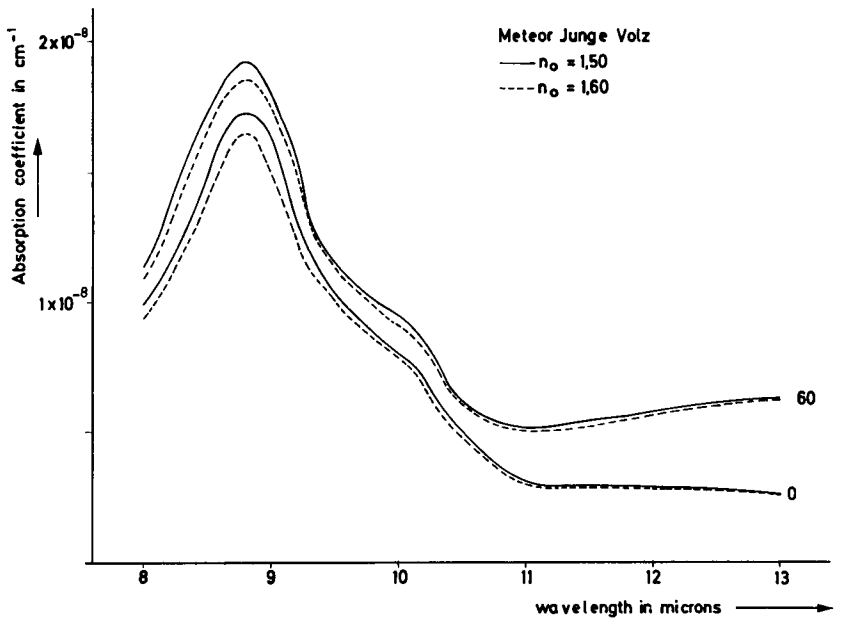

Fig. 2. Variation of the volume absorption coefficient with the real part of the refractive index n_0 for the size distribution "Meteor Junge" at 0 and 60 % relative humidity within the wavelength region of 8–13 microns.

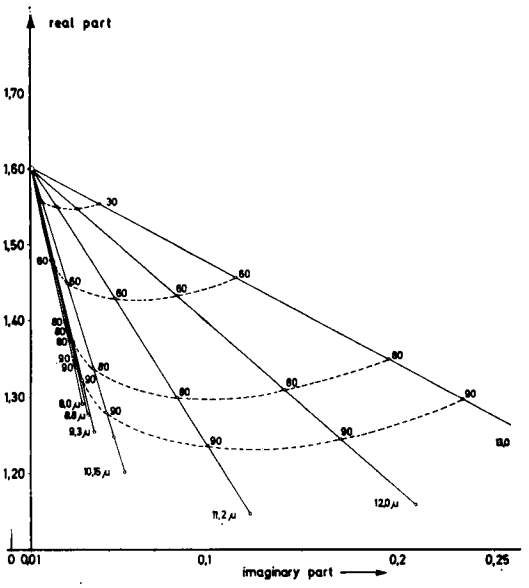

Fig. 3. Real and imaginary part of the refractive index of Haze C for different wavelengths. Numbers at the curves are relative humidites in percent. Bottom values show real and imaginary part for liquid water at different wavelengths as indicated. These bottom values will be taken by cloud particles at 100 % relative humidity. The imaginary part was arbitrarily chosen to be 0.01.

tinction efficiency Q_{ext} after Penndorf (1962) for $\alpha = 2\pi r/\lambda < 1.0$ and after Deirmendjian (1960) for $\alpha > 1.0$ with a further approximation for the scattering efficiency Q_{sca} in analogy to Deirmendjian's approximation were used. Fig. 1 shows good agreement between the Mie-theory calculations and the approximation formula even for the real part of the refractive index equal to 1.5. Two sets of imaginary parts of the refractive index were chosen. The first set is after Volz (1972) for continental aerosols and the second is an earlier assumption in order to show results for lower imaginary parts. This lower value 0.02 compares fairly well with values given by Volz (1972) for sea salt within the window region. Therefore the results with an imaginary part of 0.02 can be taken for maritime aerosols. To enable comparison between different size distributions and imaginary parts all calculations were done for the same optical depth at 0.55 micron wavelength, were the influence of the imaginary part on extinction is small. The real part of the refractive index for zero percent relative humidity was chosen to be 1.60. In test calculations a variation of the real part of the refractive index had only a little influence upon the absorption coefficient within the wavelength region of 8–13

21533490, 1973, 4, Downloaded from https://onlinelibrary.wiley.com/doi/10.1111/j.2153-3490.1973.tb00622.x by MPI 348 Meteorology, Wiley Online Library on [05/07/2023]. See the Terms and Conditions (https://onlinelibrary.wiley.com/terms-and-conditions) on Wiley Online Library for rules of use; OA articles are governed by the applicable Creative Commons License

microns, where aerosol influence is comparable to water vapour influence on radiation fluxes (Fig. 2).

The particle growth with relative humidity was introduced following measurements by Hänel (1970), (1972) for the following aerosol types:

Mainz = heavily polluted industrial area.
Meteor = maritime aerosol, sampled on the Atlantic on board the German research vessel Meteor (see Jaenicke et al., 1971).

Figs. 3 and 4 show possible variations of the refractive index with relative humidity for aerosol type "Mainz". From these figures we can conclude that calculations with constant refractive index are only a first approximation. Hänel (1972) has also measured particle growth with relative humidity for a remote mountain station within Western Germany, but the general trend was similar to that of aerosols sampled at Mainz. However aerosols sampled in heavily polluted areas grow earlier than those from remote regions. All results of the flux divergence presented for the aerosol type "Mainz" will therefore be somewhat higher than for aerosols from remote regions.

Figs. 5–7 demonstrate the strong influence of the imaginary part and relative humidity on the single scattering albedo and the extinction coefficient and therefore on the absorption coefficient of aerosols. For high relative humidities the imaginary part is mainly due to liquid water and the influence of the refractive index of dry aerosols decreases. This implies that aerosol particles with nearly no absorption coefficient at dry conditions may well be absorbing within the infrared region when growing with relative humidity.

All scattering effects were neglected since in all calculations the aerosol optical depth within the window region did not exceed 0.1. In separate calculations, using the extinction coefficient in the exponential of equation (2) instead of the absorption coefficient for aerosols, the longwave flux divergence caused by aerosols was only changed by about 10 percent thus giving an indication that neglection of scattering effects has no great influence upon flux divergence at an aerosol optical depth below 0.1.

Table 2. *Aerosol cooling rates for different atmospheres, optical depths, relative humidities for Haze C, particle growing type Mainz and imaginary parts after Volz (1972)*

Relative humidity in percent	Aerosol optical depth at 0.55 microns wavelength	Height (m)	Radiative cooling °C/day	Radiative cooling Percent of water vapour cooling
US Standard Atmosphere 1962, aerosol scale height 500 m				
30	0.4	25	0.237	8.0
	0.4	120	0.195	7.0
	0.4	220	0.161	5.5
	0.4	750	0.057	3.5
60	0.4	25	0.361	12.3
	0.4	120	0.273	9.2
	0.4	220	0.220	7.3
	0.4	750	0.076	4.7
80	0.4	25	0.450	16.9
	0.4	120	0.379	13.7
	0.4	220	0.322	11.6
	0.4	750	0.130	8.2
90	0.4	25	0.737	28.0
	0.4	120	0.622	22.2
	0.4	220	0.530	18.0
	0.4	750	0.219	13.0
Arctic atmosphere, 75° N, January, aerosol scale height 500 m				
	0.4	100	0.124	31.0
	0.4	300	0.096	15.4
	0.4	1 750	0.043	3.0
	0.2	100	0.068	15.7
	0.2	300	0.050	8.0
	0.2	1 750	0.023	1.6
Tropical atmosphere, 15° N, aerosol scale height 1 200 m				
	0.2	100	0.056	2.02
	0.2	300	0.052	2.20
	0.2	900	0.041	1.37
	0.2	2 200	0.019	0.92
	0.4	100	0.111	4.02
	0.4	300	0.101	4.32
	0.4	900	0.081	2.70
	0.4	2 200	0.039	1.85

Results

The longwave flux divergence caused by different aerosols ranges from 0.1 to 0.7°C/day for the lowest few hundred meters. Most of the values presented in Table 2 are for 0.4 optical depth at 0.55 microns and at 60 % relative humidity, values which are mean values for instance within the region of Mainz (Western

21533490, 1973, 4, Downloaded from https://onlinelibrary.wiley.com/doi/10.1111/j.2153-3490.1973.tb00622.x by MPI 348 Meteorology, Wiley Online Library on [05/07/2023]. See the Terms and Conditions (https://onlinelibrary.wiley.com/terms-and-conditions) on Wiley Online Library for rules of use; OA articles are governed by the applicable Creative Commons License

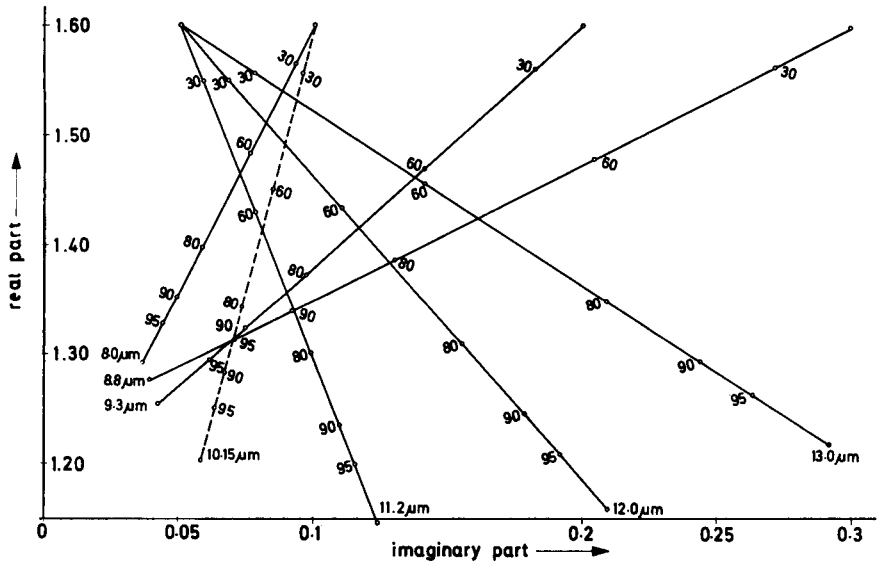

Fig. 4. Same as Fig. 3 except for imaginary parts of the refractive index for dry aerosols after Volz 1972).

Germany). A doubling of the optical depth nearly doubles cooling rates since the optical depth due to aerosols in the infrared is low, i.e. approximate values at different optical depths can be simply calculated. Occasional values of 0.7 for the optical depth in the visible would

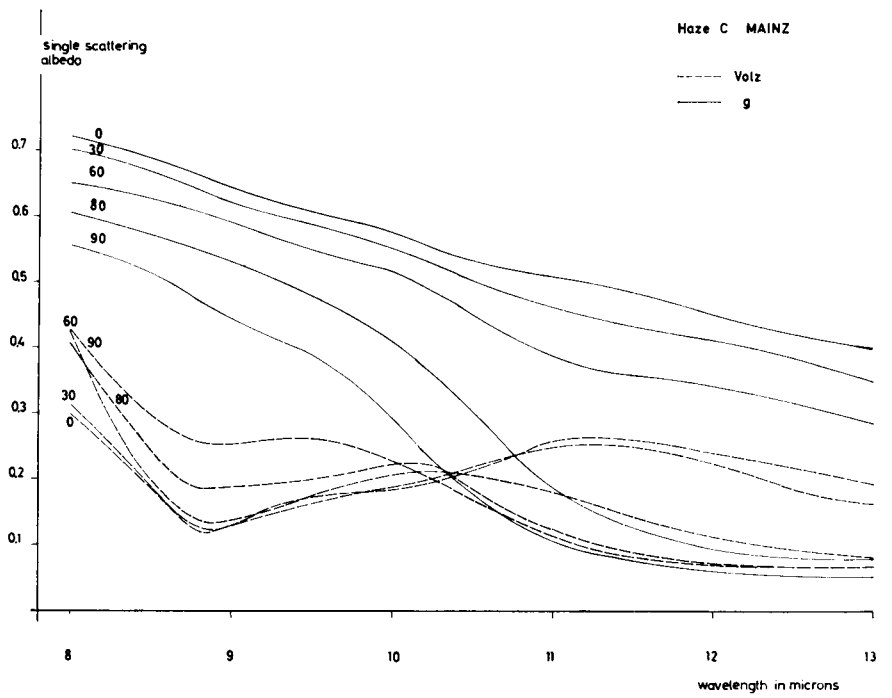

Fig. 5. Variation of the single scattering albedo with wavelength for Haze C and particle growing type "Mainz". Numbers at curves refers to relative humidity in percent. Dashed curves are for imaginary parts of the refractive index after Volz (1972), full lines for a constant imaginary part of 0.02 (low).

21533490, 1973, 4, Downloaded from https://onlinelibrary.wiley.com/doi/10.1111/j.2153-3490.1973.tb00622.x by MPI 348 Meteorology, Wiley Online Library on [05/07/2023]. See the Terms and Conditions (https://onlinelibrary.wiley.com/terms-and-conditions) on Wiley Online Library for rules of use; OA articles are governed by the applicable Creative Commons License

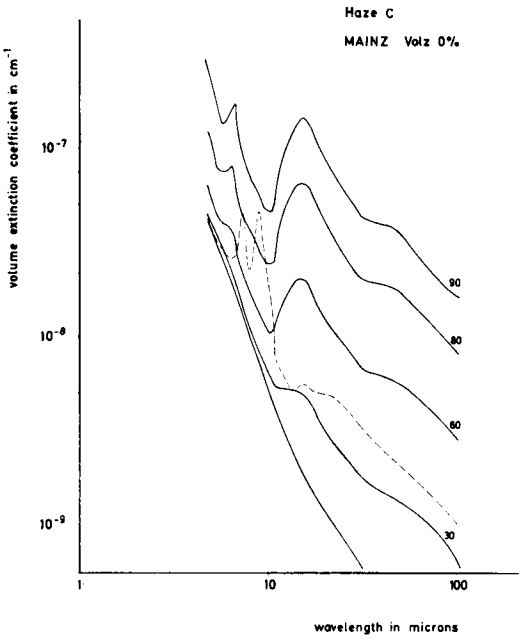

Fig. 6. Volume extinction coefficient as a function of wavelength and relative humidity as indicated at the curves. Full lines for constant imaginary part 0.02 (low). Dashed line for imaginary parts after Volz (1972).

increase aerosol contribution to radiative cooling within the lowest layers to 0.6°C/day at 60 % relative humidity. Another aerosol scale height of 1 200 meters, a proposed mean value, will reduce aerosol contribution to the lowest layers but the overall contribution would not change appreciably.

Fig. 8 shows the wavelength dependence of radiative cooling rates. Only from 8–13 microns is the aerosol contribution important thus simplifying the computations. For a very strong haze as used by Zdunkowski (1972) the net flux at a distinct height changes by more than a few percent as compared to clear skies. For instance the net flux at the ground is reduced by 3 % at 0.4 optical depth in the visible and 60 % relative humidity compared to an aerosol free atmosphere.

Since strong pollution and temperature inversions are frequently correlated, another model with a temperature inversion and all the aerosol trapped below this inversion was adopted. Particle number is constant from bottom to top. The temperature increase from 500 to 600 meters above ground was chosen to be 3°C, relative humidity was 60 % at the ground increasing

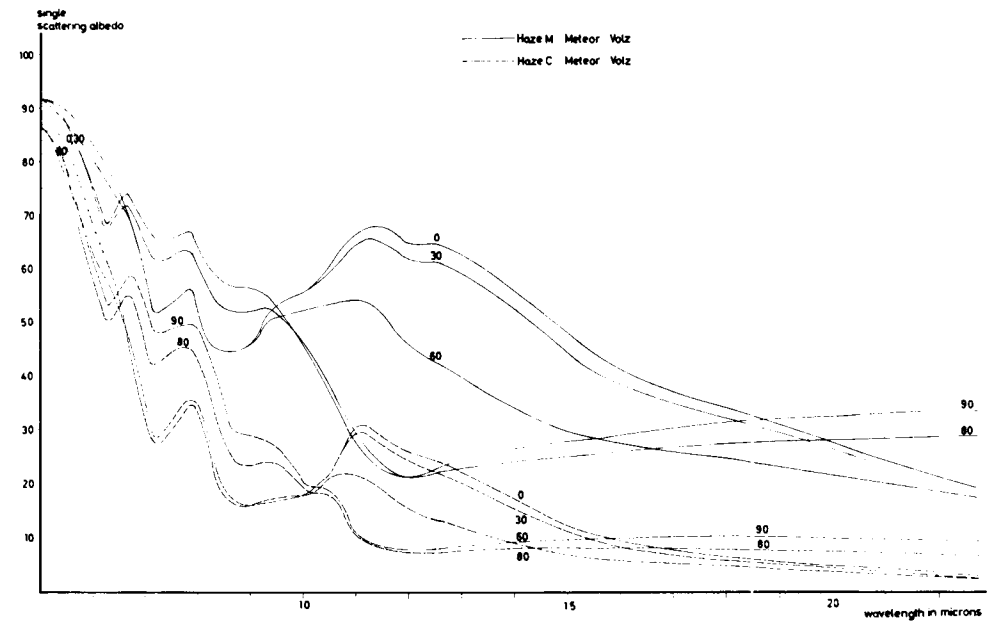

Fig. 7. Influence of particle size distribution on the single scattering albedo, for Haze M and C and equal imaginary parts; particle growing type "Meteor".

21533490, 1973, 4, Downloaded from https://onlinelibrary.wiley.com/doi/10.1111/j.2153-3490.1973.tb00622.x by MPI 348 Meteorology, Wiley Online Library on [05/07/2023]. See the Terms and Conditions (https://onlinelibrary.wiley.com/terms-and-conditions) on Wiley Online Library for rules of use; OA articles are governed by the applicable Creative Commons License

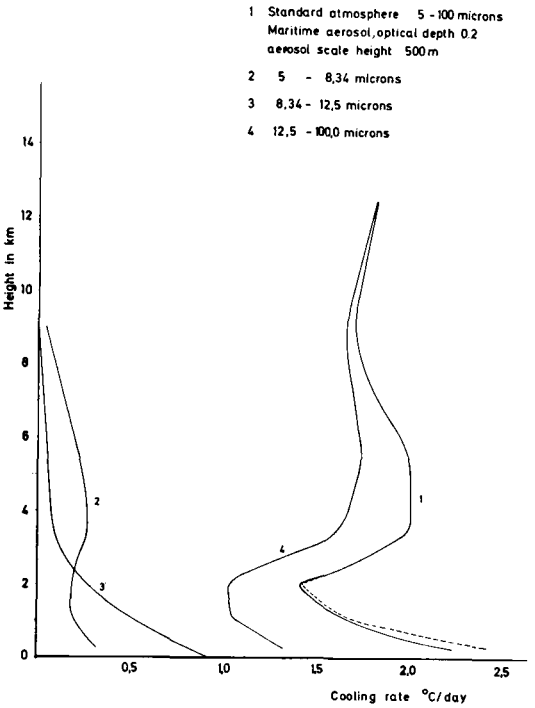

Fig. 8. Height dependence of the cooling rate for different wavelength regions. The dashed curve is for cooling by water vapour + aerosol.

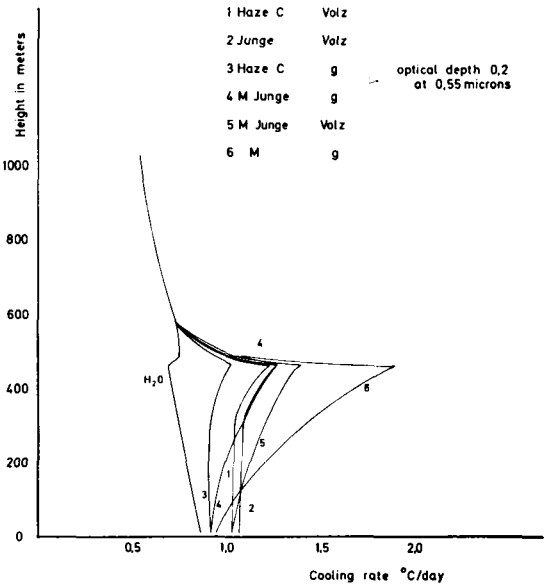

Fig. 9. Height dependence of the cooling rate for different aerosol types and imaginary parts of the refractive index (Volz, low) at equal optical depth 0.2 at 0.55 microns. The wavelength region is 8–13 microns. All aerosol particles are below 500 m with relative humidity increasing from 60 to 90 % from ground to 500 m. Particle growing type is "Mainz".

linearly to 90 % at 500 m. The temperature profile below 500 m followed the US-Standard-Atmosphere. The cooling rates due to aerosols displayed in Figs. 9 and 10 and Table 3 show a marked peak just below 500 m.

We can generally find a strong dependence on the imaginary part, relative humidity and variations of the size distribution. In Figs. 9 and 10 calculations were only performed for the window region of 8–13 microns to accelerate computing. The values given in the row "percent of water vapour cooling" in Table 3, however, correspond to total water vapour cooling within the wavelength region 5–100 microns. As can be seen from Fig. 9 a strong haze (optical depth 0.6) can lead to aerosol cooling rates just below the temperature inversion equal to those caused by water vapour. Aerosol layers tend to stabilize already existing temperature inversions. The temperature profile, however, becomes more unstable below the inversion causing a stronger mixing of the lower layers.

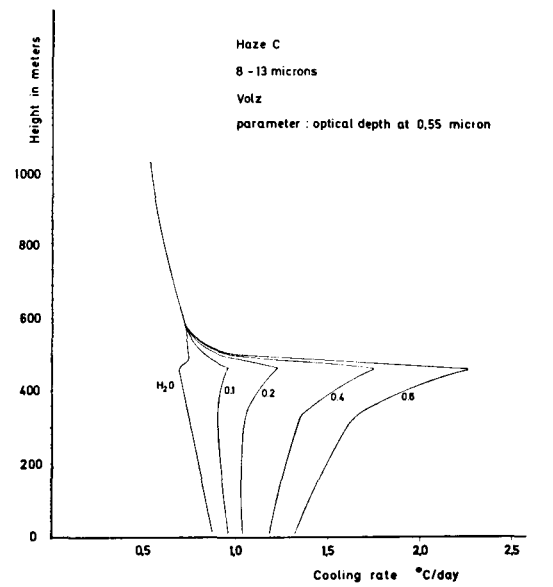

Fig. 10. Height dependence of the cooling rate for Haze C at different optical depths plus cooling by water vapour as indicated at the curves. Particle growing type is "Mainz".

21533490, 1973, 4, Downloaded from https://onlinelibrary.wiley.com/doi/10.1111/j.2153-3490.1973.tb00622.x by MPI 348 Meteorology, Wiley Online Library on [05/07/2023]. See the Terms and Conditions (https://onlinelibrary.wiley.com/terms-and-conditions) on Wiley Online Library for rules of use; OA articles are governed by the applicable Creative Commons License

Table 3. *Aerosol contribution to longwave flux divergence*

Optical depth 0.2 at 0.55 microns and 60 % relative humidity, temperature inversion at 500 m height, 60 % relative humidity at bottom, 90 % at top

Aerosol type	Imaginary part	Particle growth	Cooling rate in °C/day		Percent of water vapour cooling	
			Bottom	Top	Bottom	Top
Haze C	Volz	Mainz	0.17	0.52	7.1	23.6
Haze C	Low	Mainz	0.05	0.33	2.1	15.0
Haze M	Volz	Meteor	0.19	1.46	7.9	66.5
Haze M	Low	Meteor	0.07	1.20	2.9	54.5
Junge	Volz	Mainz	0.19	0.56	7.9	25.4
Junge	Low	Mainz	0.06	0135	2.5	15.9
M Junge	Volz	Meteor	0.16	0.70	6.7	31.8
M Junge	Low	Meteor	0.05	0.57	2..	26.0

Conclusions

At least in heavily polluted or naturally hazy areas cooling rates caused by atmospheric aerosol particles should be incorporated into general circulation models for all forecast ranges exceeding some days. Aerosol contribution to radiative cooling is believed to reduce discrepancies between measured and calculated cooling rates in the lower layers of the atmosphere (see Cox, 1969). Special attention should be drawn to all regions where temperature inversions acting as particle traps occur. If relative humidity is higher than 80 % there is an appreciable contribution even from aerosols with low absorption coefficients under dry conditions.

As a next step a comparison of heating (see Eschelbach, 1972) and cooling by aerosols in different latitudes and seasons with different albedos of the ground is planned to get a first insight into the question, whether increasing aerosol particle numbers will cause heating or cooling of the lower layers of the atmosphere.

Acknowledgement

This study was mainly supported by a grant of the Deutsche Forschungsgemeinschaft. The author's sincere appreciation is extended to Professor H. Hinzpeter for his valuable advice.

REFERENCES

1. Atwater, M. A. 1971. Radiative effects of pollutants in the atmospheric boundary layer. *J. Atm. Sci. 28*, 1367–1373.
2. Bignell, K. J., Saiedy, F. & Sheppard, P. A. 1963. On the atmospheric infrared continuum. *J.O.S.A. 53*, 466–479.
3. Bignell, K. J. 1970. The water-vapour infrared continuum. *Quart. J. Roy. Met. Soc. 96*, 390–403.
4. Cox, St. K. 1969. Observational evidence of anomalous infrared cooling in a clear tropical atmosphere. *J. Atm. Sci. 26*, 1347.
5. Deirmendjian, D. 1960. Atmospheric extinction of infrared radiation. *Quart. J. Roy. Met. Soc. 86*, 371–381.
6. Eschelbach, G. 1972. Der Einfluss des Dunstes auf den Strahlungshaushalt der Atmosphäre im sichtbaren Spektralbereich; Sonderheft zur Tagung des Verb. Deutscher Meteorol. Gesellschaften, Essen 1971. *Ann. Meteorol.*, in press.
7. Fischer, K. 1970. Measurements of absorption of visible radiation by aerosol particles. *Contr. Atm. Physics 43*, 244–254.
8. Hänel, G. 1970. Die Grösse atmosphärischer Aerosolteilchen als Funktion der relativen Feuchtigkeit. *Contr. Atm. Physics 43*, 119–132.
9. Hänel, G. 1972. The ratio of the extinction coefficient to the mass of atmospheric aerosol particles as a function of the relative humidity. *Aerosol Science 3*.
10. Jaenicke, R., Junge, C. & Kanter, H. J. 1971. Messungen der Aerosolgrössenverteilung über dem Atlantik. *Meteor Forschungsergebnisse Reihe B, No. 7*, 1–54.
11. Joseph, J. H. 1971. Thermal radiation fluxes near the sea surface in the presence of marine haze. *Israel Journal of Earth-Sciences 20*, 7–12.

21533490, 1973, 4, Downloaded from https://onlinelibrary.wiley.com/doi/10.1111/j.2153-3490.1973.tb00622.x by MPI 348 Meteorology, Wiley Online Library on [05/07/2023]. See the Terms and Conditions (https://onlinelibrary.wiley.com/terms-and-conditions) on Wiley Online Library for rules of use; OA articles are governed by the applicable Creative Commons License

12. Penndorf, R. B. 1962. Scattering and extinction coefficients for small absorbing and non-absorbing aerosols. *J.O.S.A. 52*, 896–904.
13. Rodgers, C. D. & Walshaw, C. D. 1966. The compulation of infrared cooling rate in planetary atmospheres. *Quart. J. Roy. Met. Soc. 92*, 66.
14. Rodgers, C. D. 1967. The use of emissivity in atmospheric radiation calculations. *Quart. J. Roy. Met. Soc. 93*, 43–54.
15. Volz, F. 1972. Infrared absorption by atmospheric aerosol substances. *J. of Geoph. Res. 77*, 1017.
16. Waldram, J. M. 1945. Measurement of the photometric properties of the upper atmosphere. *Quart. J. Roy. Met. Soc. 71*, 319–336.
17. Zdunkowski, W. G. & McQuage, N. D. 1972. Short-term effects of aerosol on the laye near the ground in a cloudless atmosphere. *Tellus 24*, 237–254.

ВЛИЯНИЕ АЭРОЗОЛЯ НА РАДИАЦИОННОЕ ВЫХОЛАЖИВАНИЕ

Частицы аэрозоля имеют комплексной показатель преломления и поэтому дают вклад в излучение атмосферы и скорости радиационного выхолаживания. В данной статье представлены результаты расчетов дивергенции потока длинноволнового излучения в атмосфере на различных высотах с учетом водяного пара и аэрозольных частиц как излучателей и поглотителей. Спектральная область простирается от 5 до 100 микрон и подразделяется на 23 спектральных интервала. Необходимые свойства аэрозольных частиц — альбедо единичного рассеяния и коэффициент экстинкции были вычислены сначала по теории Ми, а затем по приближенной формуле Фольца с комплексным показателем преломления. Учитывался также рост частиц с относительной влажностью для аэрозолей различного типа и с разными распределениями частиц по размерам. Эти величины были взяты из данных Хэнела. Результаты указывают на значительный вклад аэрозольных частиц в дивергенцию потока длинноволнового излучения, хотя этот вклад сильно зависит от мнимой части коэффициента поглощения, распределения частиц по размерам и от относительной влажности. Вклад аэрозоля в радиационное выхолаживание становится очень важным в слоях под инверсиями температуры, которые являются барьерами для диффузии частиц. Существуют атмосферные условия, когда вклад аэрозоля в радиационное выхолаживание становится таким же большим, как выхолаживание, благодаря водяному пару.

21533490, 1973, 4, Downloaded from https://onlinelibrary.wiley.com/doi/10.1111/j.2153-3490.1973.tb00622.x by MPI 348 Meteorology, Wiley Online Library on [05/07/2023]. See the Terms and Conditions (https://onlinelibrary.wiley.com/terms-and-conditions) on Wiley Online Library for rules of use; OA articles are governed by the applicable Creative Commons License